ORIGINAL ARTICLE

Plastic anisotropic and damage evolution analysis of recycled aluminium alloy AA6061 at high rate of strain

C. S. Ho[1], M. K. Mohd Nor[1*], M. A. Ab Rani[1], N. Ma'at[1], M. T. Hameed Sultan[2] and M. A. Lajis[3]

[1] Crashworthiness and Collisions Research Group (COLORED), Mechanical Failure Prevention and Reliability Research Centre (MPROVE), Faculty of Mechanical and Manufacturing Engineering, Universiti Tun Hussein Onn Malaysia, 86400 Batu Pahat, Johor, Malaysia
[2] Department of Aerospace Engineering, Faculty of Engineering, Universiti Putra Malaysia, 43400 Serdang, Selangor Malaysia
[3] Sustainable Manufacturing and Recycling Technology (SMART), Advanced Manufacturing, and Material Centre (AMMC), Faculty of Mechanical and Manufacturing Engineering, Universiti Tun Hussein Onn Malaysia, 86400 Batu Pahat, Johor, Malaysia

ABSTRACT – Aluminium alloys have been widely used in many applications, and its usage is increasing yearly due to its distinctive properties. Nevertheless, it required high energy consumption and pollution during the production of primary sources. This leads to the attention in producing secondary sources to substitute the primary aluminium. Recycling of aluminium alloys adopted in automotive structures is a great option to save thousands of energy and prevent tons of CO_2 from being released to the atmosphere. Numerous investigations must be conducted to establish the mechanical behaviour before the specific applications can be identified. However, there is a challenge for such recycled aluminium to achieve the same application as the primary sources due to material properties degradation related to damage. It is still an open study area to be explored for a better understanding of the behaviours of recycled aluminium. Thus, in this work, the Taylor Cylinder Impact test is used to investigate anisotropic-damage behaviour of recycled aluminium alloy AA6061 undergoing high-velocity impact from 190m/s to 300 m/s using two length-to-diameter (L/D) ratios. The recovered samples are observed under an optical microscope (OM) and scanning electron microscope (SEM). A strong strain rate dependency can be seen as the damage evolution is increasing as the impact velocity increase. Further, the corresponding digitized footprints analysis exhibit plastic anisotropic and localized plastic strain in such recycled material. This can be clearly observed from the development of a non-symmetrical footprint within the impact surface. This test is the first to explore the deformation behaviour of recycled materials using high-velocity cylinder impact in a high rate of strain deformation regime.

INTRODUCTION

Aluminium alloys are a standout amongst and most well-known material for some application and products in the market as it has many benefits. There is a considerable measure of sorts, of aluminium. For pure aluminium combinations, it has delicate and low-quality properties so with a specific end goal to improve its quality, others components, for example, Magnesium (Mg), Silicon (Si), Copper (Cu), Zinc (Zn), Lithium (Li) and Manganese (Mn) are included and mixed into an aluminium synthesis [1]. One of the most used high-strength materials in automotive application is aluminium Al-Mg-Si AA6061 alloy. The chemical composition and mechanical properties of the AA6061 is shown in Table 1 [2]. It was reported that the usage of such aluminium in a car could reduce CO_2 emission and benefit on fuel-saving [3]. The high demand for the aluminium has led to a production shortage. Extracting aluminium from bauxite ore is an energy-consuming process. The production of primary aluminium is 4,927 thousand metric tons in September 2017. Based on the data observations, the demand for the aluminium is very high that requires high energy for the extraction process. Therefore, to save energy, recycling aluminium is extremely encouraged which can save about 95% of energy. This situation leads to the production of recycling aluminium. In recycling aluminium, two methods are conventional and direct conversion recycling methods. In the direct conversion recycling method, the hot press forging technique proved that this method has good potential can bring benefits whether in terms of enhancement of metals properties or environmental [4].

Recycling aluminium had been well-explored and widely used in the automotive structure as it is a great option to save energy and reduce the release of CO_2. Also, many investigations had been conducted to establish the mechanical behaviour before the specific applications can be identified [5]. Nevertheless, there is a challenge for such recycled aluminium to achieve the same application as the primary aluminium source as there is degradation of the material properties related to damage [6]. Thus, it is vital to understand the deformation behaviour of a material associated with damage undergoing finite strain deformation. It can enforce a limitation on the potential application and failure of the design if without a better understanding of the particular topic.

Table 1. Chemical composition and mechanical properties of AA6061 [2]

Chemical Composition / Elements	Content, (%)	Mechanical Properties	Value
Al	97.8	Ultimate Tensile Strength (UTS)	310 MPa
Si	0.62		
Mg	0.87	Young Modulus (E)	68.9 GPa
Fe	0.16		
Cu	0.32	Yield Strength	276 MPa
Mn	0.02		
Cr	0.09	Elongation at break	17%
Zn	0.12	Density	2.7 g/cc
Ti	<0.01	Vickers Hardness	107

Damage can be characterized as an accumulation of lasting microstructural changes adjusting thermo-mechanical properties (e.g., solidness, quality, anisotropy, and so forth) and acquire an arrangement of irreversible physical micro-cracking forms due to the utilization of thermo-mechanical loading [7]. In aluminium composites, damage can be identified with advancing microstructural highlights such as scanning electron microscope (SEM), optical microscope (OM), etc. The failure mechanism in ductile materials is related to the nearby failure of second stage particles, incorporations, intermetallic particles, and precipitates. For instance, [8] demonstrated that the splitting of particles in A357 aluminium composite happens amid plastic deformation.

In addition, Balasundaram et al. [9] have proposed that damage in aluminium compounds is created by breaking of intermetallic particles, development of voids at broke particles and void mixture. The investigation verified that the heading of breaks under pressure loading was opposite to the heap course. Along these lines, the approach for distinguishing damage of aluminium composite is essential for evaluating parts lifespan in the car, aviation, hardware, and other metal-based industries. It should be noted that the damage is numerously related to the basic reaction of the material microstructure subjected to various loading conditions. The deformation behaviour of such anisotropic materials under dynamic shock loading has been discussed extensively in various works, see for example [10–16]. Besides, related works examining the anisotropic influence on material behaviour undergoing finite strain deformation and shock waves can be found in [17,18]. In this research, high-velocity impact test is adopted as an essential approach to investigate the damage progression. The field of impact progression covers various circumstances and is important to engineers from different distinctive areas. For instance, production engineers are keen regarding the matter in regards to its application to rapid blanking and opening flanging forms while vehicle makers utilize their comprehension of the reaction of structures to impact loading to enhance the functionality and safety of their items. Notwithstanding, high-velocity impact essentially centered on primary metals explored by numerous analysts. Conversely, the recycling metals experience high-velocity impact to a great extent unexplored. Most materials demonstrated considerable changes in the mechanical reaction under expanded rates of stressing [19, 20].

In the field of crash and impact modelling, many experimental works can be utilized to test the impact deformation of the material such as Taylor impact test, Split Hopkinson Pressure Bar test, Dynamic Tensile Extrusion test, Gravitational Drop-weight test, and others. However, the Taylor impact test is the most common and usually adopted to determine the material properties and strain rate dependent on the scope of dynamic deformation due to its simplicity and the potential in determining the yield behaviour at high strain-rates [21]. Taylor cylinder impact test can be regarded as one of the best approaches to investigate damage progression under high-velocity impact. The test is named after G. I. Taylor who developed the test to screen materials in ballistic applications during WWII [22]. This test entails firing a solid cylinder rod of material under consideration, typically 7.5 to 12.5 mm in diameter by 25 to 40 mm in length, at high velocity against a massive and plastically rigid target. Taylor cylinder impact testing has previously been utilized to probe both the deformation responses of metals and alloys in the presence of large gradients of stress, strain and strain-rate and as a means to validate constitutive models [21, 23]. This axis-symmetric integrated test provides a readily conducted experimental method to examine the large-strain high-strain rate mechanical behaviour of materials, at the same time evaluating the accuracy of appropriate "physics" incorporation in constitutive models [24]. It is simple, inexpensive, and exhibits large strains, high-strain rates at elevated temperatures. In this study, the Taylor cylinder impact test is adopted to examine damage evolution in Taylor specimens due to high shock pressures and plastic strains during the test. The deformable flat-nosed cylinders are fired against a fixed quasi-rigid wall that allows for material behaviour estimation at high-strain rates, and the damage evolution of the specimen is described based on the deformation elastoplasticity behaviour of the specimen. The elastoplasticity behaviour of the specimen can be refer to the deformed mushrooming-shaped specimen, where the specimen can be divided into two parts separated by an elastic-plastic interface: (i) mushrooming zone near the impact end where plastic deformation occurred, and (ii) undeformed zone at the rear end that

described by back and forth movement of elastic wave [25]. The mushrooming is also defined as plastic deformation, radial expansion and reduction in length without any visible cracks. When the impact velocity exceeds the material's limit, the mushrooming deformation might evolve to another fracture mode. Further detailed associated with fracture mode are defined in Rakvåg et al. [26] and Rakvåg et al. [27].

In short, aluminium alloy has outstanding applications and the primary sources have become depleted day by day and an alternative for secondary sources (recycled aluminium alloy) is needed to replace the primary sources. In fact, recycled aluminium alloy has several damages that can lead to the failure of the materials. Before an application is applied, the damage behaviour of the material is important as any object could occur impact or collide with another body in real life. Thus, in this study, the plastic anisotropic and damage behaviour of the recycled AA6061 is evaluated via the Taylor impact test.

SPECIMEN PREPARATION

Figure 1 represents the process flow of the test specimen preparation. A vertical center CNC machine (MAZAK Nexus 410A-II CNC Mill) is used for chips production with an average chips size of 5.2 mm x 1.097 mm x 0.091 mm using 377 m/min of cutting speed.

The chips then are cleaned with Acetone solution using an ultrasonic bath and dried in a 60°C thermal oven. Subsequently, the hot press forging technique is applied to form the recycled specimen. The process is performed at 530°C and 47 MPa (35.6 tonnes) with 2 hours holding time, including four times the pre-compacting cycle [28]. Subsequently, the specimen is quenched at 100°C/s quench rate to perform rapid cooling into ambient temperature, and then artificial aging at 175°C thermal oven for 120 minutes. The final specimen is then denoted as T5-temper. The electrical wire cutting machine is eventually used to form a symmetrical cylinder specimen shaped, as shown in Figure 2.
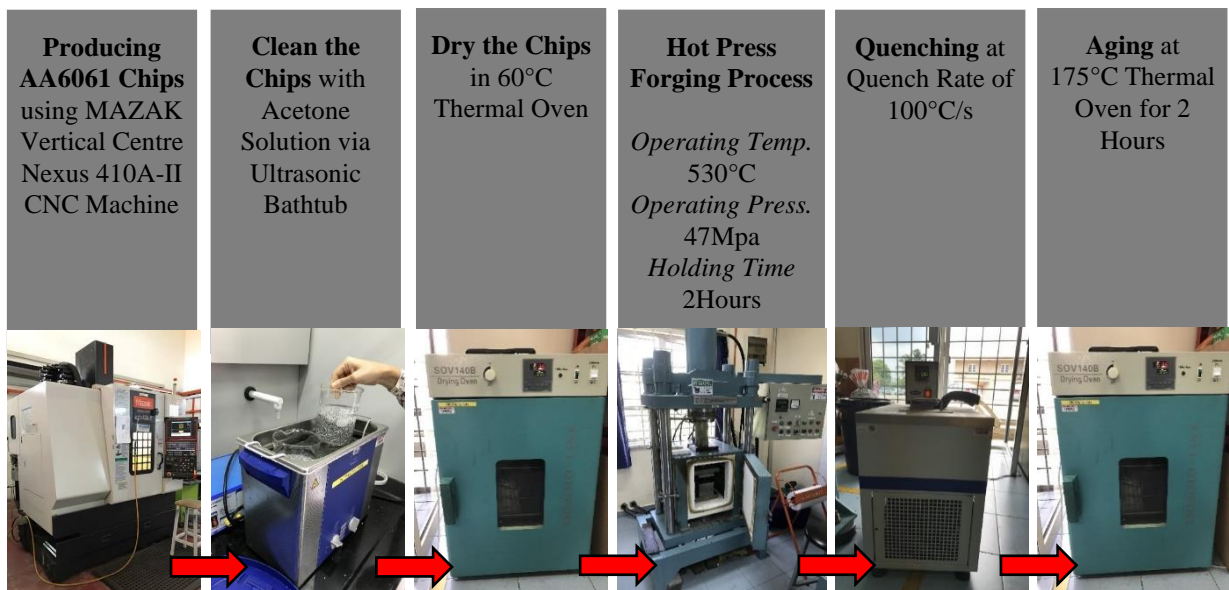

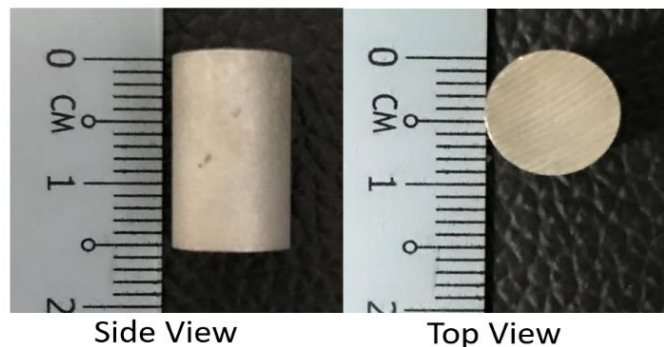**Figure 1.** Process flow of specimen preparation

Figure 2. Cylindrical shaped specimen

EXPERIMENTAL IMPLEMENTATION

The Taylor cylinder impact test is conducted by launching a cylindrical specimen from a smooth bored gun barrel to the rigid massive hardened stainless-steel target. To ensure the effect of friction is ignorable, the target surface is polished to a mirror-like finished. The recycled aluminium alloy specimens are prepared into two different L/D ratios: 1.25 and 1.75, with the corresponding length ±10.55 mm and ±14.75 mm, respectively. Both L/D ratios set with the same diameter ±8.45 mm. The pressure and specimen size are selected based on the limitation of the gas gun machine. Table 2 shows the test matrix for this impact test. Figure 3 shows the arrangement of the impact gas gun machine used in this research.

First, the bullet specimen is inserted into the gas gun tunnel, and pressure is used as a force to launch the bullet toward the target. After the bullet is launched, a high-speed camera is utilized to capture the movement of the bullet towards the target. The impact velocity is then measured and calculated based on the video captured. The deformation behaviour of the specimen is observed. Eventually, the specimens are cold-mounted, grind, polished, and etching for observation under SEM. It should be noted that enough energy is required by the specimen to hit the target, and generate permanent plastic deformation. Once plastic deformation is obtained, the data is valid for analysis. This plastic deformation behaviour can be clearly observed around the footprint of the impact surface, as compared to the initial footprint. Therefore, in this work, a minimum pressure was first identified and validated in the preliminary test. An adequate energy is also important to avoid too much wobbling of the specimen.
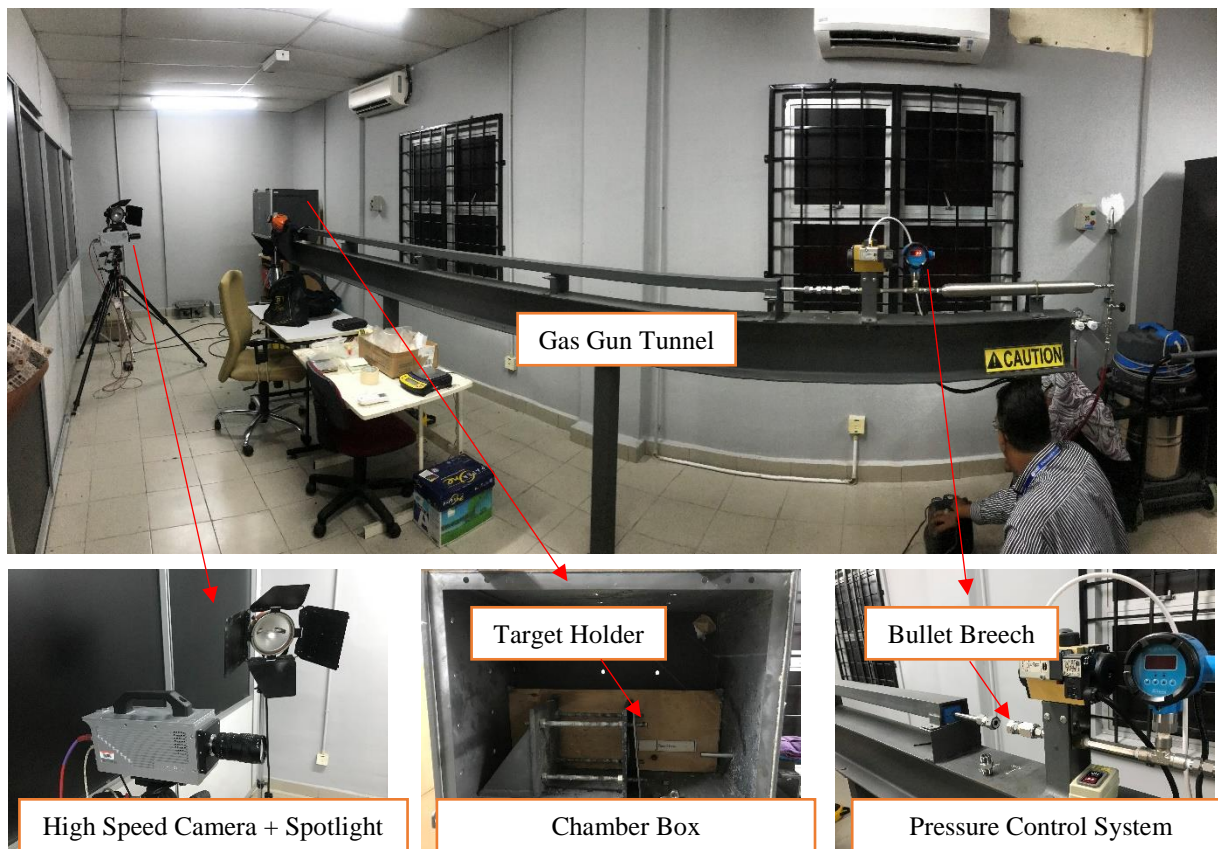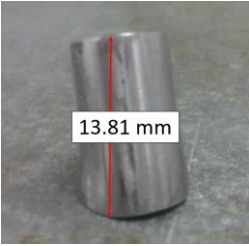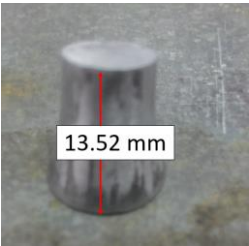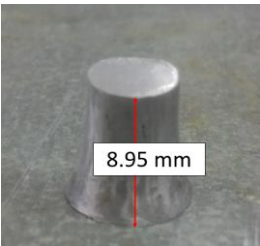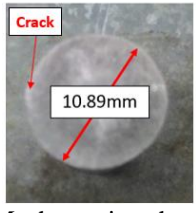

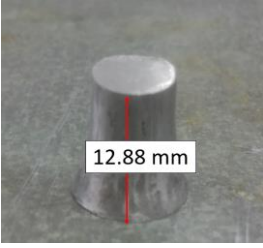**Figure 3.** Impact gas gun machine

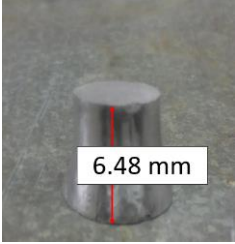**Table 2.** Test matrix for Taylor cylinder impact test

Pressure (Bar)	L/D	Length, L (mm)	Diameter, D (mm)	Remark
6	1.75	14.75	8.45	A1
	1.25	10.55	8.45	B1
10	1.75	14.75	8.45	A2
	1.25	10.55	8.45	B2
15	1.75	14.75	8.45	A3
	1.25	10.55	8.45	B3

RESULTS AND DISCUSSIONS

The experimental results are shown in Table 3. First, it can be seen that the specimen with a lower L/D ratio produces higher velocity compared to the one with a higher L/D ratio, due to the contained mass. However, the localized plastic strain deformation is less severe referring to the maximum diameter measured around the footprint. The largest and the smallest diameter are obtained in the recovered specimens A3 and B1, respectively. Figure 4 shows the SEM micrograph of specimens A1 and B1 that tested at pressure 6 bar (velocity range from 190 – 210 m/s). This figure shows that an obvious influence of significant localized plastic strain deformation is due to the growth of cracks and voids propagation. As can be seen, the number of voids that are leading to micro-cracks (damage evolution) is increasing in the recovered specimen A1 (higher L/D ratio) compared to B1 (lower L/D ratio).

Table 3. Result of Taylor impact test

Remark	Velocity (m/s)	Side Profile	Footprint/ Fracture Mode
A1	193.13	13.81 mm	10.60mm Mushrooming shape
B1	206.25	9.73 mm	10.36mm Mushrooming shape
A2	228.65	13.52 mm	12.16mm Mushrooming shape
B2	235.15	8.95 mm	Crack 10.89mm Mushrooming shape with crack around the edge

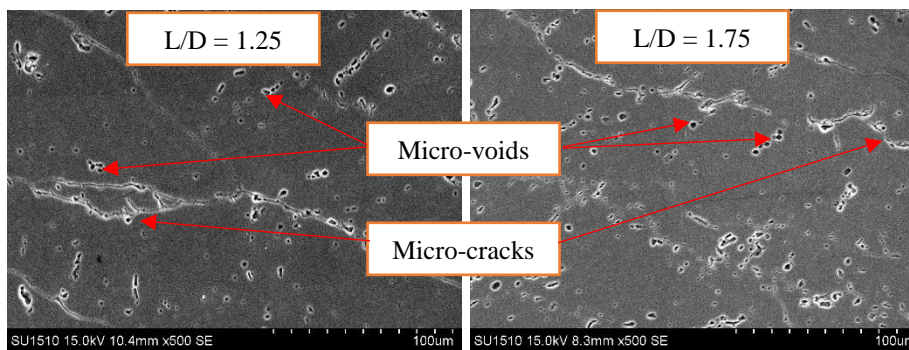| Remark	Velocity (m/s)	Side Profile	Footprint/ Fracture Mode
A3	247.85	12.88 mm	Mushrooming shape with crack around the edge
B3	273.00	6.48 mm	Mushrooming shape with an obvious crack

Figure 4. SEM micrographs of specimen A1 (L/D 1.25) and B1 (L/D 1.75)

Generally speaking, the results show a strong plastic anisotropic of the recycled AA6061 undergoing finite strain deformation. This is observable from an ellipse (non-symmetrical) footprint of the post-specimens. In addition, a ductile fracture is clearly observed by a mushrooming shape development within the recovered specimens driven by voids initiation, growth and coalescence. No visible exterior cracks can be seen unless in specimens B2, A3 and B3 of Table 3. Figure 5 and Figure 6 illustrate the OM micrograph of specimen A1 and A2, respectively. These figures show that the fracture occurs around the edge of the footprint (Figures 5(a) and 6(a) while crack initiation and void evolution start at the center of the specimen (Figures 5(b), 5(c) and 6(b), 6(c)). This indicates crack is progresses due to localized plastic strain expand radially from the center to the edge of footprint. Some factors that affect the dynamic growth of void such as heat generated by plastic deformation, inertial effects associated with displacement and wave interactions [19]. It can be observed that the damage at the edge of the A2 footprint is severer than experienced by A1 which is proportional to the impact velocity for A2 and A1; 228.65 m/s and 193.13 m/s, respectively, due to the damage development of voids initiation, growth and coalescence that leading into cracks during the deformation.
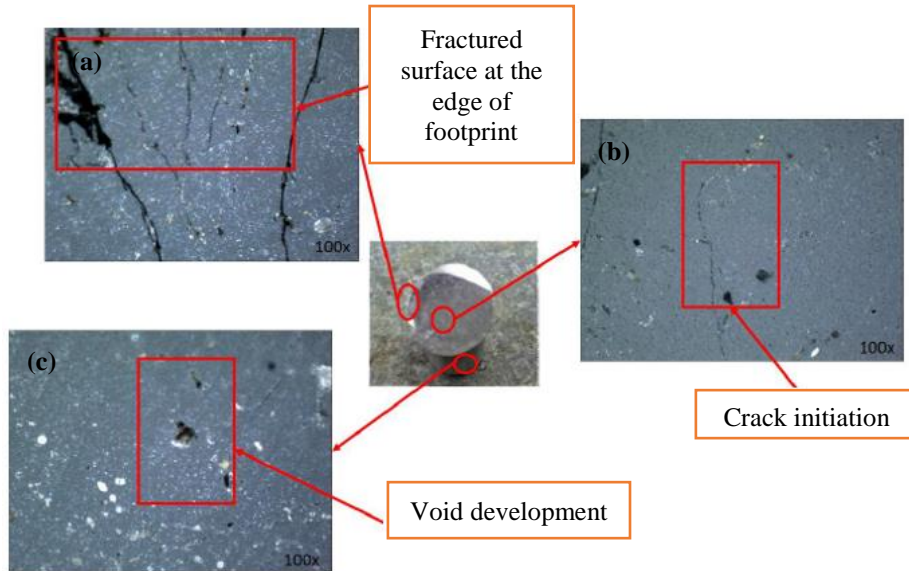
Figure 5. Optical microscope analysis on footprint of specimen A1: (a) edge, (b) crack initiation, and (c) void development
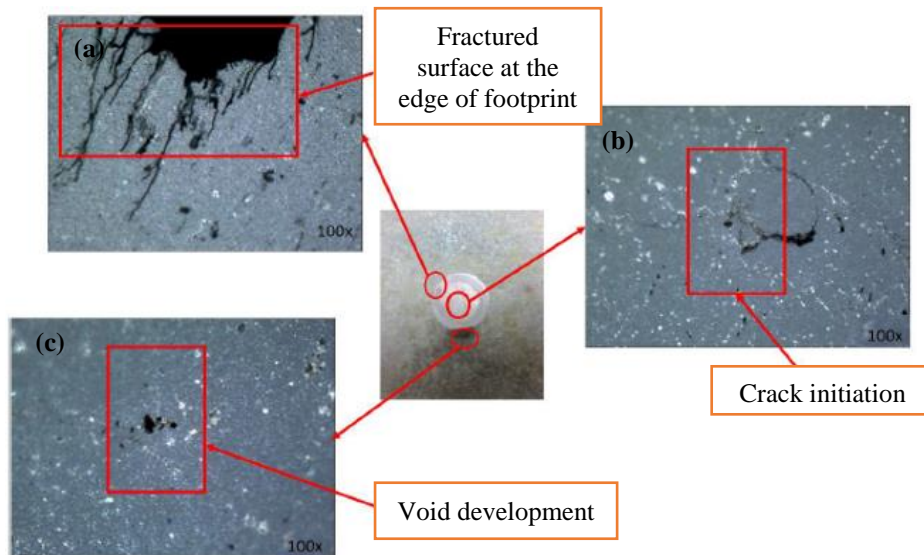

Figure 6. Optical microscope analysis on footprint of specimen A2: (a) edge, (b) crack initiation, and (c) void development

Figure 7 shows the corresponding SEM analysis of specimens A1 and A2. The pre and post micrographs are provided to examine damage development in the specimens deeply. Ductile fracture is clearly observed driven the damage development. First, voids can be seen initiated in the test specimen of the recycled AA6061 nucleated during the specimen's preparation. The voids grow and coalesce further during the impact to form many more voids leading to result in micro-cracks in the specimen as shown in this figure. Also, the specimens show strong strain rate dependency as the damage evolution is increasing as the impact velocity increases cause severe localized plastic strain deformation as observed in the footprint radial expansion.
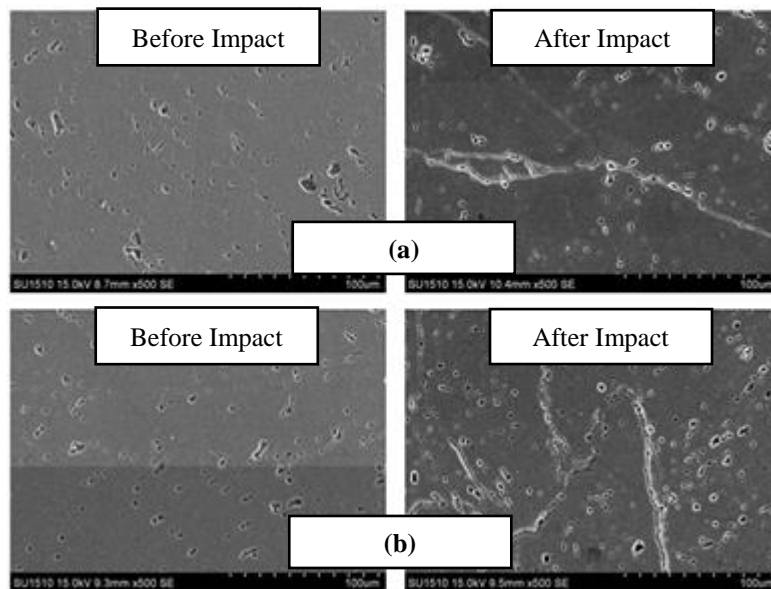
Figure 7. SEM micrographs of specimen: (a) A1 and (b) A2, before and after impact

Figure 8 depicts side profiles of the sample of the specimen with a high L/D ratio (L/D= 1.75), which impacted at v= 247.85 m/s (Specimen A3). It can be observed that the length of the specimen reduced from an initial length of 14.75 mm to about 10.75 mm, and a radial expansion from an initial diameter of 8.45 mm to approximately 12.88 mm. Another example with the L/D ratio of 1.25, impacted at v= 235.15 m/s (Specimen B2), is shown in Figure 9. There is also a reduction in length from 10.55 mm to about 8.95 mm and expansion in diameter from 8.45 mm to 10.89 mm. The radial expansion can be noticed clearly in the digitized footprint plotted in Figure 10.

By referring to Figure 8 and Figure 9, it can be seen that the digitized side profiles exhibited severe mushrooming shape, and the footprint expands non-symmetrically (ellipse shape footprint), as shown in Figure 10. This confirms the plastic anisotropy of such recycled material. As an exhibit in other ductile materials, the mushrooming shape only develops in a certain region from the footprint as the reflected wave of plastic strain ceases in the middle of the specimen. As depicted in Figures 8 and 9, the geometrical changes of side profiles stop at approximately 6 mm and 8mm from the footprint (impact surface), respectively. This indicates that the plastic strain energy is more significant at higher impact velocity, but still can be fully absorbed by the specimens even having low L/D ratios.

In addition, the deformed footprint that develops a non-symmetrical ellipse-shaped is depicted by the black colour line in Figure 10. As aforementioned, this is due to plastic anisotropic characteristics and localized plastic strain around the impact surface. In the event of an impact, the footprint of anisotropic materials experiences different responses in various directions within the impact surface. It can be seen in Figure 10 that the deformed footprint shows a different value along the x-axis and z-axis for both the specimen A3 and B2. Again, this is due to the different mechanical properties in different directions of such material. It seems the same response sustains in the recycled form of aluminium alloys AA6061.
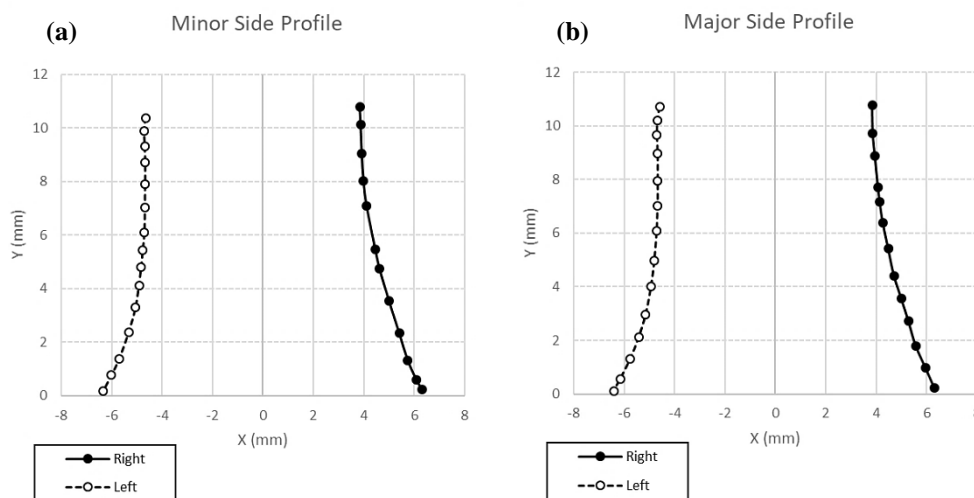

Figure 8. Major and minor side profiles for post-test geometry A3 (v= 247.85 m/s): (a) minor side profile and (b) major side profile
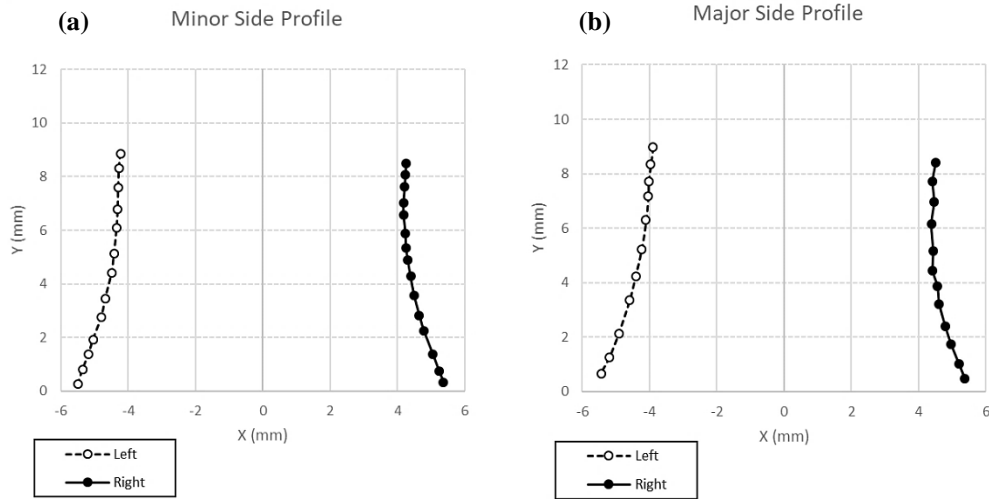
Figure 9. Major and minor side profiles for post-test geometry B2 (v= 235.15 m/s): (a) minor side profile and (b) major side profile
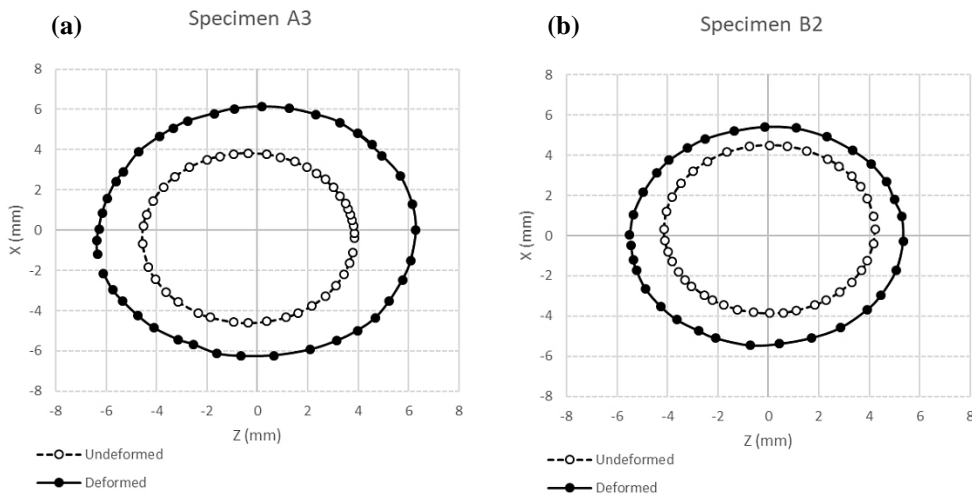

Figure 10. Digitized footprints for specimen: (a) A3 (v=247.85 m/s) and (b) B2 (v=234.15 m/s)

CONCLUSIONS

This paper investigates the anisotropic-damage behaviour in the recycled aluminium alloy AA6061 undergoing high-velocity impact using the Taylor cylinder impact test. From the deformed specimen, a non-symmetrical ellipse locus of the footprint is shown by such recycled AA6061, which pronounced anisotropic behaviour of such material undergoing finite strain deformation. The impact velocity is influenced by the pressure applied and also the weight or L/D ratio of the specimen. The higher the impact velocity, the radial expansion on the impact surface is getting larger. The critical impact velocity of such recycled AA6061 is found to be lower than 235 m/s. Cracks form around the edge of the impact surface after exceeding the critical impact velocity.

Moreover, from the observation of the microscopic analysis, it showed the value of impact velocity directly influences the void growth. Further, the void progression and ductile damage seem been affected by the void developed within the impact area, as shown in the microscopic analysis. The microstructural comparison between pre and post-test samples reveals the location of the fracture happened at the very edge of the impact face. First, it must be emphasized that the recycled specimen of AA6061 exhibit ductile fracture, which strong dependent on microstructure. It can be seen that damage development in both L/D ratios is significantly influenced by void initiation, growth and coalescence specifically within the impact surface. This damage evolution is leading to the radial expansion of impact surface and reduction in specimen length. The microstructural comparison between pre and post-test specimens reveals the mechanism. This analysis proves that the difference in microstructural properties leads to variation in the failure mechanism.

ACKNOWLEDGMENTS

REFERENCES

[1]   N. K. Yusuf, M. A. Lajis, and A. Ahmad, "Hot Press as a Sustainable Direct Recycling Technique of Aluminium : Mechanical Properties and Surface Integrity," *Materials (Basel).*, vol. 10, no. 8, p. 902, 2017.

[2]   J. Hirsch, B. Skrotzki, and G. Gottstein, *Aluminium Alloys: The Physical and Mechacnial Properties, Volume 1*, 1st ed. John Wiley & Sons, Inc., 2008.

[3]   S. N. A. Rahim, M. A. Lajis, and S. Ariffin, "Effect of Extrusion Speed and Temperature on Hot Extrusion Process of 6061 Aluminum Alloy Chip," *ARPN Journal of Engineering and Applied Sciences*, vol. 11, no. 4, pp. 2272–2277, 2016.

[4]   A. Ahmad, M. A. Lajis, N. K. Yusuf, and A. Wagiman, "Hot Press Forging as the Direct Recycling Technique of Aluminium - A Review," *ARPN Journal of Engineering and Applied Sciences*, vol. 11, no. 4, pp. 2258–2265, 2016.

[5]   A. Ahmad, M. A. Lajis, N. K. Yusuf, S. Shamsudin, and Z. W. Zhong, "Parametric Optimisation of Heat Treated Recycling Aluminium (AA6061) by Response Surface Methodology," in *AIP Conference Proceedings*, 2017, vol. 1885, no. 1, pp. 1–7.

[6]   E. Tillová, M. Chalupová, and L. Hurtalová, "Evolution of Phases in a Recycled Al-Si Cast Alloy during Solution Treatment," in *Scanning Electron Microscopy*, V. Kazmiruk, Ed. IntechOpen, 2012, pp. 411–438.

[7]   S. Castagne, A. Habraken, and S. Cescotto, "Application of a Damage Model to an Aluminium Alloy," *International Journal of Damage Mechanics.*, vol. 12, no. 1, pp. 5–30, 2003.

[8]   B. Wan, W. Chen, T. Lu, F. Liu, Z. Jiang, and M. Mao, "Review of Solid State Recycling of Aluminum Chips," *Resources, Conservation & Recycling*, vol. 125, pp. 37–47, 2017.

[9]   A. Balasundaram, A. M. Gokhale, S. Graham, and M. F. Horstemeyer, "Three-dimensional Particle Cracking Damage Development in an Al-Mg-base Wrought Alloy," *Materials Science and Engineering: A* vol. 355, no. 1–2, pp. 368–383, 2003.

[10]   M. D. Furnish and L. C. Chhabildas, "Alumina Strength Degradation in the Elastic Regime," *AIP Conference Proceedings*, vol. 429, no. 1, pp. 501–504, 1998.

[11]   R. Minich, J. Cazamias, M. Jumar, and A. Schwartz, "Effect of Microstructural Length Scales on Spall Behaviour of Copper," *Metall. Mater. Trans. A*, vol. 35, no. 9, pp. 2663–2673, 2004.

[12]   J. D. Colvin, R. W. Minich, and D. H. Kalantar, "A model for plasticity kinetics and its role in simulating the dynamic behavior of Fe at high strain rates," *International Journal of Plasticity*, vol. 25, no. 4, pp. 603–611, 2009.

[13]   G. I. Kanel, E. B. Zaretsky, A. M. Rajendran, S. V. Razorenov, A. S. Savinykh, and V. Paris, "Search for Conditions of Compressive Fracture of Hard Brittle Ceramics at Impact Loading," *International Journal of Plasticity*, vol. 25, no. 4, pp. 649–670, 2009.

[14]   A. S. Khan and C. S. Meredith, "Thermo-Mechanical Response of Al 6061 with and without Equal Channel Angular Pressing (ECAP)," *International Journal of Plasticity*, vol. 26, no. 2, pp. 189–203, 2010.

[15]   E. B. Zaretsky and G. I. Kanel, "Plastic Flow in Shock-Loaded Silver at Strain Rates from 10^4 s^-1 to 10^7 s^-1 and Temperature from 296 K to 1233 K," *Journal of Applied Physics*, vol. 110, no. 7, p. 073502, 2011.

[16]   C. S. Meredith and A. S. Khan, "Texture Evolution and Anisotropy in the Thermo-Mechanical Response of UFG Ti Processed via Equal Channel Angular Pressing," *J. Plast.*, vol. 30–31, pp. 202–217, 2012.

[17]   A. S. Khan, R. Kazmi, and B. Farrokh, "Multiaxial and Non-proportional Loading Responses, Anisotropy and Modeling of Ti-6Al-4V Titanium Alloy Over Wide Ranges of Strain Rates and Temperatures," *International Journal of Plasticity*, vol. 23, no. 6, pp. 931–950, 2007.

[18]   M. K. M. Nor, R. Vignjevic, and J. Campbell, "Modelling of Shockwave Propagation in Orthotropic Materials," *Applied Mechanics and Materials*, vol. 315, pp. 557–561, 2013.

[19]   V. Panov, "Modelling of Behaviour of Metals at High Strain Rates," Ph.D. Thesis, Cranfield University, 2006.

[20]   C. S. Ho *et al.*, "Characterization of Anisotropic Damage Behaviour of Recycled Aluminium Alloys AA6061 Undergoing High Velocity Impact," *International Journal of Integrated Engineering*, vol. 11, no. 1, pp. 247–256, 2019.

[21]   C. A. Acosta, C. Hernandez, and A. Maranon, "Validation of Material Constitutive Parameters for the AISI 1010 Steel from Taylor Impact Tests," *Materials & Design*, vol. 110, pp. 324–331, 2016.

[22]   G. Taylor, "The Use of Flat-Ended Projectiles for Determining Dynamic Yield Stress. II. Tests on Various Metallic Materials," *Proceedings of The Royal Society A Mathematical, Physical and Engineering Sciences*, vol. 194, no. 1038, pp. 300–322, 1948.

[23]   P. J. Maudlin, J. F. Bingert, J. W. House, and S. R. Chen, "On the Modeling of the Taylor Cylinder Impact Test for Orthotropic Textured Materials: Experiments and Simulations," *International Journal of Plasticity.*, vol. 15, no. 2, pp. 139–166, 1999.

[24]   H. Lim, J. D. Carroll, C. C. Battaile, S. R. Chen, A. P. Moore, and J. M. D. Lane, "Anisotropy and Strain Localization in Dynamic Impact Experiments of Tantalum Single Crystals," New Mexico, USA, 2018.

[25] S. Chakraborty, A. Shaw, and B. Banerjee, "An Axisymmetric Model for Taylor Impact Test and Estimation of Metal Plasticity," *Proceedings of the Royal Society of London Series A*, vol. 471, p. 20140556, 2015.

[26] K. G. Rakvåg, T. Børvik, I. Westermann, and O. S. Hopperstad, "An Experimental Study on the Deformation and Fracture Modes of Steel Projectiles during Impact," *Materials & Design.*, vol. 51, pp. 242–256, 2013.

[27] K. G. Rakvåg, T. Børvik, and O. S. Hopperstad, "A Numerical Study on the Deformation and Fracture Modes of Steel Projectiles during Taylor Bar Impact Tests," *International Journal of Solids and Structures*, vol. 51, no. 3–4, pp. 808–821, 2014.

[28] A. Ahmad, M. A. Lajis, and N. K. Yusuf, "On the Role of Processing Parameters in Producing Recycled Aluminum AA6061 Based Metal Matrix," *Materials (Basel).*, vol. 10, no. 1098, pp. 1–15, 2017.